RSC Advances

ROYAL SOCIETY OF CHEMISTRY

www.rsc.org/advances

RSC Advances

ARTICLE

High-performance supercapacitors based on graphene/MnO_2/activated carbon fiber felt composite electrodes in different neutral electrolytes

Received 00th January 20xx,
Accepted 00th January 20xx

DOI: 10.1039/x0xx00000x

www.rsc.org/

Qian Yang[a, b], Liubing Dong[a, b], Chengjun Xu[a*] and Feiyu Kang[a, b*]

Graphene/MnO_2 composites are introduced into activated carbon fiber felt (ACFF) to fabricate composite textile electrodes. Their micro-structure, electrical property and electrochemical performance for supercapacitor applications in different neutral electrolytes (1M $NaNO_3$ and $Ca(NO_3)_2$ aqueous solutions) have been studied. The composite electrodes have similar pore features to original ACFF textiles, but show notably enhanced electrical and electrochemical performances. The composite textile electrodes show low electrical resistance, high specific capacitance (up to 1516 mF/cm^2 in neutral electrolytes) and excellent cycling stability (no capacitance decay after 5000 charge-discharge cycles). Besides, electrochemical capacitance of composite textile electrodes in $Ca(NO_3)_2$ electrolyte is higher than that in $NaNO_3$ electrolyte at low scan rates (1-5 mV/s), but the situation is reversed when scan rates are higher than 10 mV/s. Above all, the results show that our low-cost composite textile electrodes are high-performance in neutral electrolytes, which is helpful for developing large-scale energy storage devices.

1. Introduction

Supercapacitors, also known as electrochemical capacitors, have fast charge-discharge rate, high power capability and long cycle lifetime.[1-6] Supercapacitors have been used in a wide range of applications such as portable electric devices, hybrid cars, intelligent wireless sensors and memory backup systems.[7-11] However, limited energy density, usually lower than batteries by an order of magnitude, hinders broader applications of supercapacitors.[7] During the past years, a significant amount of effort has been devoted to improve the energy density of supercapacitors.[12-16] MnO_2 is one type of transition-metal oxides and has high specific pseudocapacitance due to reversible redox reactions near the surface.[17-21] However, because of its poor electrical conductivity, MnO_2 has low rate capability and stability, and broader applications of MnO_2 are still a great challenge.[18, 22] Graphene (GN), a two-dimensional carbon material, has advantages of good electronic conductivity, high specific surface area and high chemical stability.[23-26] Due to expectation to combine their merits together, various GN/MnO_2 composites have been synthesized and explored.[22, 27-31] We put forward a self-reacting micro-emulsion method to prepare ultrathin amorphous MnO_2 nanosheets with high capacitance of over 500 F/g in Na_2SO_4 electrolyte.[32, 33] This method can be utilized to prepare GN/MnO_2 composites.

In our previous work, activated carbon fiber felt (ACFF) was used to prepare multiscale carbon composite textiles and all-carbon compressible supercapacitors.[34] However, the high-performance supercapacitors were achieved in a strong alkaline electrolyte (6M KOH aqueous solution), this may increase risk of environmental issues.

In this work, GN/MnO_2 composites prepared through self-reacting micro-emulsion method were introduced into ACFF to fabricate GN/MnO_2/ACFF composite textile electrodes. Micro-structure, electrical property and electrochemical performance of the prepared GN/MnO_2/ACFF composite electrodes in different neutral electrolytes were studied. The composite electrodes have similar pore features to original ACFF but better electrochemical performance. The neutral electrolytes also eliminate the risks and environmental issues of strong alkaline electrolytes. As a whole, our results show that the cheap ACFF, modified by GN/MnO_2 composites, is capable to be used as supercapacitor electrodes in neutral electrolytes, which is helpful for developing supercapacitors with high performance and low cost.

2. Experimental

2.1 Materials

ACFF textiles, with thickness of ~3.0 mm, were purchased from Shenzhou Carbon Fiber Co., Ltd, China. Water-based GN paste (Model: Pas2002, 5.49 wt%) was obtained from SuperC (Dongguan) Technology Co., Ltd, China. The AR grade potassium permanganate ($KMnO_4$), sodium bis (2-ethylhexyl) sulfosuccinate (Aerosol-OT, AOT), isooctane, sodium nitrate

[a] Graduate School at Shenzhen, Tsinghua University, Shenzhen 518055, China.
[b] School of Materials Science and Engineering, Tsinghua University, Beijing 100084, China.
E-mail address: vivaxuchengjun@163.com (C. Xu)
fykang@mail.tsinghua.edu.cn (F. Kang)

($NaNO_3$) and calcium nitrate ($Ca(NO_3)_2$) were purchased from Sinopharm Chemical Reagent Co., Ltd.

2.2 Synthesis of GN/MnO_2/ACFF composite textiles

Firstly, GN/MnO_2 composites were synthesized through self-reacting micro-emulsion method. AOT was excessive and all added $KMnO_4$ was reduced to MnO_2 in this method, so the weight of MnO_2 could be calculated. 17.11 g (or 1.07 g) GN paste was added into 500 ml 0.1M AOT/isooctane solution followed by 30-minute ultrasound. 27 ml 0.1M $KMnO_4$ aqueous solution was added into the suspension followed by an-hour ultrasound. The product (dark brown precipitate) was separated, washed with ethanol and deionized water and dried at 80 ℃ for 12 h. The product was denoted as 80GM (or 20GM) (the weight ratio of GN to MnO_2 was 80: 20 (or 20: 80)). Then 0.25 g 80GM (or 20GM) was dispersed in 50 ml deionized water by sonifier cell disrupting for 2 h. A wafer-shaped piece of ACFF, with diameter of 15 mm, was immersed in the 80GM (or 20GM) suspension and then freeze-dried. The obtained GN/MnO_2/ACFF composite textile electrodes were denoted as 80GMC (or 20GMC). Weight of ACFF, 20GMC and 80GMC is 21.2 mg, 21.5 mg and 21.7 mg respectively.

2.3 Characterization

Weight of all textile electrodes was measured on an electronic balance. Their micro-structures were observed through scanning electron microscopy (SEM. Model: Hitachi, S-5200). Electrical conductivity was measured on a four-point probe instrument. The specific surface area and pore size distribution were measured on Micromeritics ASAP2020 analyzer. Specific surface area (S_{BET}) and total pore volume (V_p) were determined by BET method and single point adsorption, respectively.

2.4 Electrochemical measurement

To measure the electrochemical performances of our composite textile electrodes, full-cell symmetric supercapacitors were assembled. 1M $NaNO_3$ or $Ca(NO_3)_2$ aqueous solution was used as the electrolyte. Supercapacitors in which the electrolyte is $NaNO_3$ and the electrode is ACFF, 20GMC and 80GMC were denoted as ANa, 20Na and 80Na, respectively. Similarly, those in $Ca(NO_3)_2$ electrolyte were denoted as ACa, 20Ca and 80Ca, respectively. Electrochemical tests of cyclic voltammetry (CV) and galvanostatic charge-discharge (GCD) were performed on an Im6e (Zahner) electrochemical station. The specific capacitance of a single electrode was calculated on the area of one electrode (1.767 cm^2).

3. Results and discussion

The micro-structure of prepared GN/MnO_2 composite powder is first observed. The SEM images of 20GM and 80GM, as shown in Fig. 1, indicate that the GN/MnO_2 composites with different GN contents are successfully synthesized and MnO_2 is loaded on the GN sheets. What's more, the GN sheets in SEM images are not thin or transparent, which proves that the GN we use, is composed by several layers instead of single layer GN sheets. The product information provided by the manufacturer also confirms this.

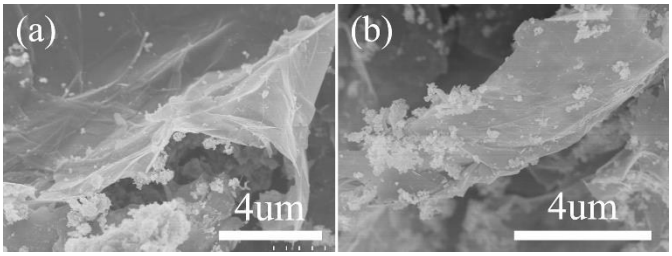

Fig. 1 SEM images of (a) 20GM, (b) 80GM.

The micro-morphology of the obtained GN/MnO_2/ACFF composite textiles is displayed in Fig. 2. Fig. 2a and b show the SEM images of ACFF textiles. The images indicate that the original ACFF is fabricated by intertwining and overlapping carbon fibers, giving rise to a great quantity of holes in different sizes in the textiles. The abundance of holes makes ACFF textiles have high specific surface area and other excellent features of foams, such as bendability and compressibility. As observed in our experiments, ACFF textiles have ultrahigh water absorbability, which makes the impregnation process much simpler and quicker than other carbon materials.[35] As shown in Fig. 2c-f, the GN/MnO_2 composites are successfully introduced into ACFF. As can be seen, GN/MnO_2 composites with different weight ratio of GN to MnO_2 are attached on the surface of activated carbon fibers. However, when GN content increases, one distinct difference is that volume of nanofillers in 80GMC becomes much more than that in 20GMC. This volume increase makes GN aggregation more serious.

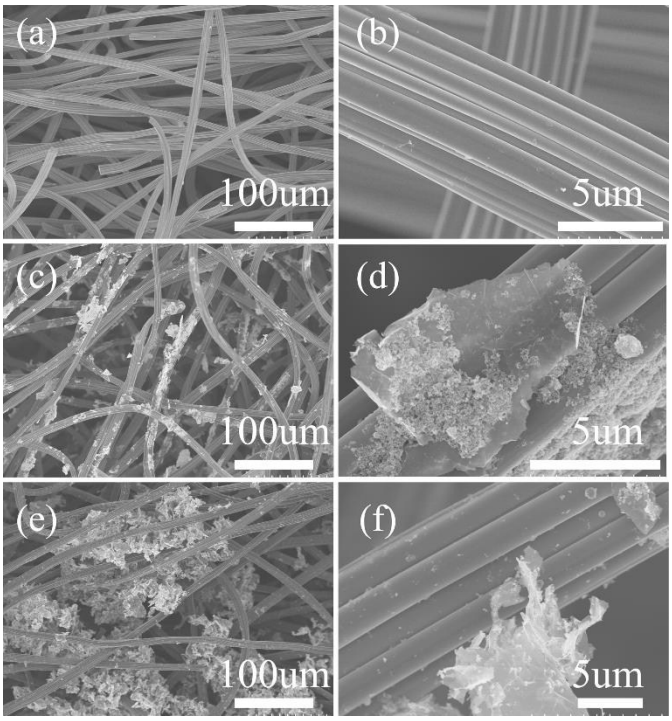

Fig. 2 SEM images of (a, b) ACFF, (c, d) 20GMC and (e, f) 80GMC.

It should be noted that in the assembled full-cell supercapacitors, the electrodes are highly compressed. In this case, GN/MnO_2 particles are pinned in local spaces encircled by carbon fibers, thus will not easily fall off the composite electrodes in supercapacitors.

Fig. 3a displays the electrical conductivity of textiles. As can be seen, conductivity is improved after introducing GN/MnO_2 composites. The electrical conductivity of 20GMC and 80GMC is 35% and 114% higher than that of ACFF, respectively. Due to the short carbon fibers used in manufacturing ACFF, as well as its porous feature, the electrical conductivity of ACFF is not as high as other carbon fabrics.[36, 37] The added GN sheets could increase the channels for electron transport. For further consideration of the compressed state of electrodes in full-cell supercapacitors, we also measured the conductivity when the textile samples are manually pressed. It is obvious that the conductivity is higher than that at fluffy state. Although the pressure on the samples cannot be measured precisely, the data does indicate that those composite textiles can achieve higher conductivity when they are used as electrodes in full-cell supercapacitors.

In previous work[34], the S_{BET}, V_p and d of ACFF were measured to be 1528 m^2/g, 0.65 cm^3/g and 1.73 nm respectively. Fig. 3b shows N_2 adsorption/desorption isotherms of 80GMC. The type I isotherms indicate the micropore structure of 80GMC.[38] The S_{BET}, V_p and d of 80GMC are 1465 m^2/g, 0.58 cm^3/g and 1.57 nm respectively. All of these figures are lower than their counterparts of original ACFF. Because the few-layered GN in our experiments has lower specific surface area than ACFF and the GN sheets can cover some pores of ACFF body materials. As shown in the inset of Fig. 3b, most pore sizes distribute under 2 nm, this reflects the micropore feature of 80GMC again.

Fig. 4a-f show CV curves of supercapacitors at scan rates of 1-20 mV/s. For ANa and ACa, the quasi-rectangular shape of CV curves only exists at low scan rates (1-2 mV/s), the deformation of CV curves becomes serious at high scan rates. This reflects the poor electrochemical performance of original ACFF. For 20Na and 20Ca, although the deformation of CV curves is not as serious as ACFF, the narrow areas of CV curves still indicate low capacitance of 20GMC. For 80Na and 80Ca, the rate performance is much better. When the scan rate increases, the CV curves of 80Na and 80Ca maintain rectangular well.

Fig. 4g displays areal capacitance of the single electrode at scan rates of 1-20 mV/s. Compared with ACFF, the capacitance of 80GMC is largely enhanced while that of 20GMC is slightly improved. For example, the specific capacitance (C_s) of ACa, 20Ca and 80Ca at 2 mV/s is 763 mF/cm^2, 918 mF/cm^2 and 1516 mF/cm^2 respectively. Besides, after introducing GN/MnO_2 composites, the capacitance retention of textile electrodes is improved. The rate performance of 80GMC is much better than ACFF, while the improvement of 20GMC is negligible. For example, when the scan rate increases from 1 mV/s to 20 mV/s, about 13.7%, 17.0% and 54.6% of C_s retains for ANa, 20Na and 80Na respectively.

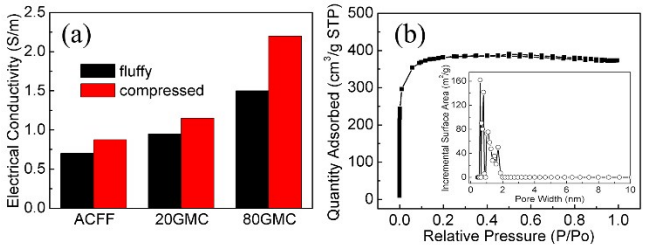

Fig. 3 (a) electrical conductivity of textiles at different states; (b) N_2 adsorption/desorption isotherms of 80GMC at 77 K (the inset of (b) exhibits the pore size distribution).

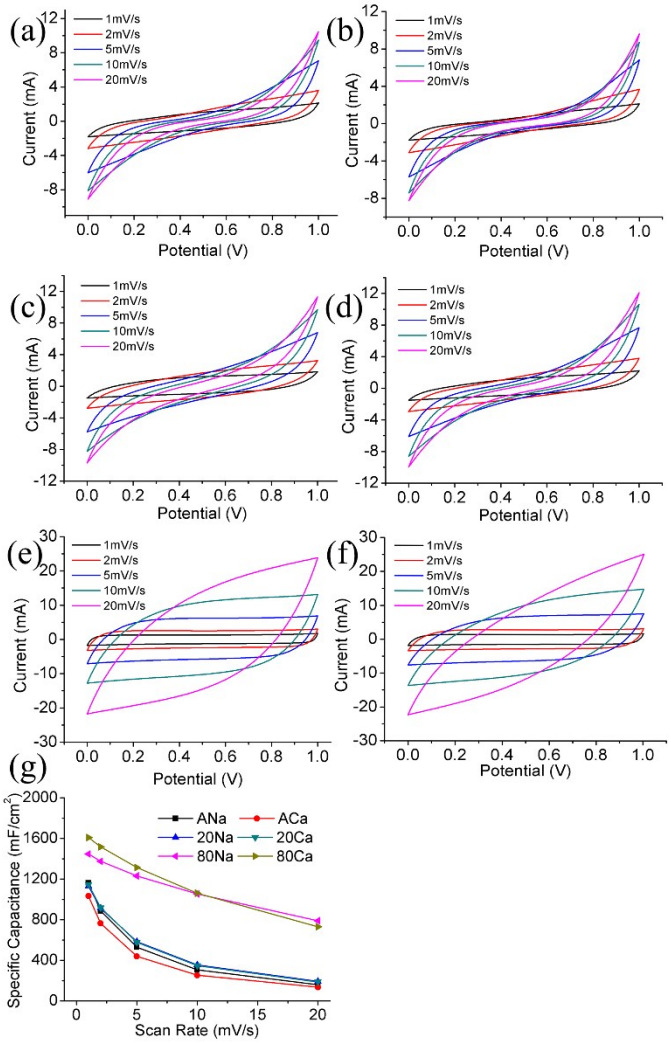

Fig. 4 CV curves at different scan rates of (a) ANa, (b) ACa, (c) 20Na, (d) 20Ca, (e) 80Na, (f) 80Ca; (g) Areal capacitance of each sample calculated from CV curves.

Different electrolytes have different influence on each textiles. For ACFF and 20GMC, the C_s and C_s retention rate between $NaNO_3$ and $Ca(NO_3)_2$ electrolytes do not show large distinction. Unlike ACFF and 20GMC, different electrolytes lead to distinguishing electrochemical performance of 80GMC. At low scan rates (1-5 mV/s), 80Ca possesses higher C_s than 80Na, while at high scan rates (10-20 mV/s), 80Ca possesses lower C_s than 80Na. Thus when the scan rate increases from 1 mV/s to 20 mV/s, the C_s retention rate of 80Ca is 9.1% lower than that of 80Na. This variation mainly results from the different capacitance of MnO_2 in $NaNO_3$ and $Ca(NO_3)_2$ electrolytes. The capacitance of MnO_2 in $Ca(NO_3)_2$ electrolyte is much higher than that in $NaNO_3$ electrolyte at 2 mV/s.[39-41] Due to this reason, the

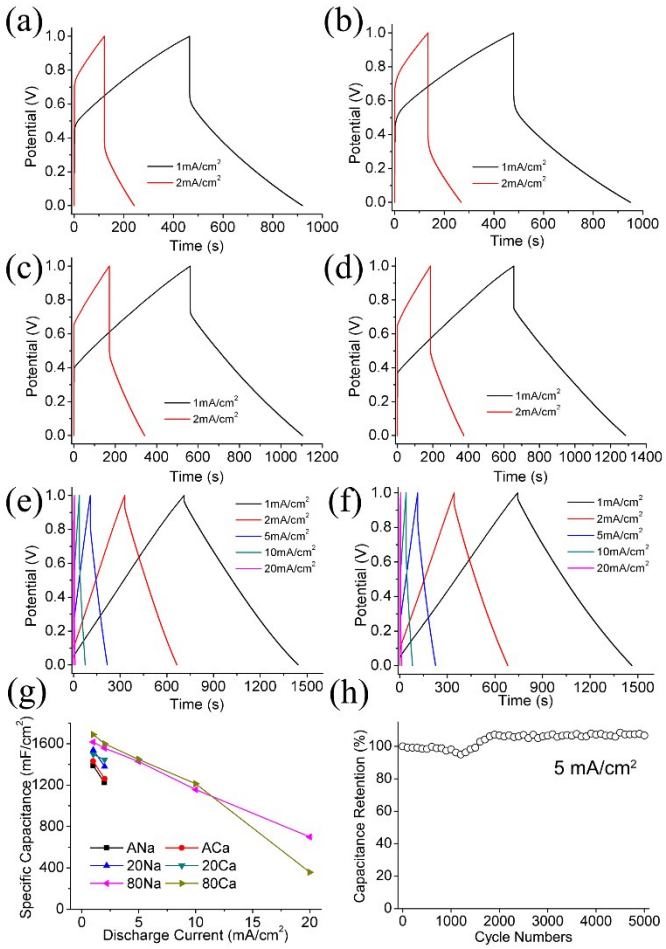

Fig. 5 GCD curves of (a) ANa, (b) ANa, (c) 20Na, (d) 20Ca, (e) 80Na, (f) 80Ca at different current densities (1-20 mA/cm^2); (g) Areal capacitance of each sample calculated from GCD curves; (h) Cycling stability of 80Ca tested at the current density of 5 mA/cm^2.

capacitance of 80Ca is higher than that of 80Na at low scan rates (1-5 mV/s). However, at high scan rates (10-20 mV/s), the cation diffusion in electrolytes has a significant impact on the electrode capacitance: compared with Na^+, Ca^{2+} has a lower diffusion coefficient and mobility, thus leading to a smaller capacitance of MnO_2. Therefore, capacitance of 80GMC electrode in $Ca(NO_3)_2$ electrolyte is lower than that in $NaNO_3$ electrolyte at high scan rates.

As shown in Fig. 5a-f, after introducing GN/MnO_2 composites, more symmetric GCD curves, longer discharging time and smaller *IR* drops are achieved, especially for 80GMC. The *IR* drop reflects internal resistance of supercapacitors. For clear comparison between different textiles, the equivalent series resistance (ESR) is used and can be calculated according to equation:

$$\mathrm{ESR} = 1000 \times \frac{IR}{2I}$$

IR (V) is the *IR* drop during discharge process, I (mA/cm^2) is the current density. ESR values of ANa, ACa, 20Na, 20Ca, 80Na and 80Ca are about 149, 150, 118, 120, 16 and 14 Ω cm^2 respectively at I=2 mA/cm^2. As can be seen, after introducing GN/MnO_2 composites, the electrical resistance of textiles decreases, while the influence of different electrolytes is negligible.

Because the high resistance of ACFF and 20GMC makes their *IR* drops theoretically larger than 1 V at the scan rate of more than 2 mA/cm^2, the charge-discharge process of them lasts less than 1 second and the C_s cannot be calculated from GCD curves. Therefore Fig. 5 only contains GCD curves and C_s of ACFF and 20GMC at 1-2 mA/cm^2. As shown in Fig. 5g, C_s has been improved after introducing GN/MnO_2 composites, and C_s of 80GMC is higher than that of 20GMC. Different electrolytes do not have much impact on the C_s of ACFF and 20GMC, but influence the electrochemical performance of 80GMC. The C_s of 80Ca is higher than that of 80Na at low current density, and decreases faster when the current density increases. So when the current density increases from 1 mA/cm^2 to 20 mA/cm^2, C_s of 80Na is retained about 43%, while that of 80Ca is retained about 23%. 80Na can achieve 25.4 μWh/cm^2 of energy density with 895.2 μW/cm^2 of power density at current density of 5 mA/cm^2. This variation of C_s calculated from GCD curves is as same as that calculated from CV curves. Long-term cycling performance of 80Ca was also evaluated. As presented in Fig. 5h, there is no capacitance decay after 5000 charge-discharge cycles, demonstrating its excellent cycling stability.

Conclusions

In this work, GN/MnO_2/ACFF composite electrodes are prepared by introducing GN/MnO_2 composites into ACFF textiles. The electrochemical performances of as-prepared composite textile electrodes in neutral electrolytes (1M $NaNO_3$ and $Ca(NO_3)_2$ aqueous solutions) are studied. After introducing GN/MnO_2 composites, lower electrical resistance and better electrochemical performances of the electrodes are observed. Besides, capacitance of composite textile electrodes in $Ca(NO_3)_2$ electrolyte is higher than that in $NaNO_3$ electrolyte at low scan rates (1-5 mV/s), but the situation is reversed when the scan rate is higher than 10 mV/s. Our results show that the low-cost composite textile electrodes are high-performance in neutral electrolytes, which is helpful for developing large-scale energy storage devices.

Acknowledgements

We would like to thank NSFC (No. 51102139 and 51232005) and Shenzhen Technical Plan Projects (No. JC201105201100A and JCYJ20130402145002425) for financial support. We also appreciate the financial support from Guangdong Province Innovation R&D Team Plan (2009010025).

Notes and references

1. A. Burke, *Journal of Power Sources*, 2000, **91**, 37-50.
2. Y. Huang, J. Liang and Y. Chen, *Small*, 2012, **8**, 1805-1834.
3. A. Burke, *Electrochimica Acta*, 2007, **53**, 1083-1091.
4. R. Kötz and M. Carlen, *Electrochimica Acta*, 2000, **45**, 2483-2498.

5. B. E. Conway, *Electrochemical supercapacitors: scientific fundamentals and technological applications*, Springer Science & Business Media, 2013.
6. X. Zhang, H. Zhang, C. Li, K. Wang, X. Sun and Y. Ma, *RSC Adv.*, 2014, **4**, 45862-45884.
7. P. Simon and Y. Gogotsi, *Nature materials*, 2008, **7**, 845-854.
8. J. R. Miller and P. Simon, *Science Magazine*, 2008, **321**, 651-652.
9. P. J. Hall and E. J. Bain, *Energy policy*, 2008, **36**, 4352-4355.
10. L. G. H. Staaf, P. Lundgren and P. Enoksson, *Nano Energy*, 2014, **9**, 128-141.
11. L. Dong, Z. Chen, D. Yang and H. Lu, *RSC Advances*, 2013, **3**, 21183.
12. J. Yan, Q. Wang, T. Wei and Z. Fan, *Advanced Energy Materials*, 2014, **4**, 1300816.
13. J. Yan, Z. Fan, W. Sun, G. Ning, T. Wei, Q. Zhang, R. Zhang, L. Zhi and F. Wei, *Advanced Functional Materials*, 2012, **22**, 2632-2641.
14. A. Izadi‐Najafabadi, S. Yasuda, K. Kobashi, T. Yamada, D. N. Futaba, H. Hatori, M. Yumura, S. Iijima and K. Hata, *Advanced Materials*, 2010, **22**, E235-E241.
15. Z. Tang, C. h. Tang and H. Gong, *Advanced Functional Materials*, 2012, **22**, 1272-1278.
16. W. Deng, X. Ji, Q. Chen and C. E. Banks, *RSC Advances*, 2011, **1**, 1171.
17. M.-W. Xu, D.-D. Zhao, S.-J. Bao and H.-L. Li, *Journal of Solid State Electrochemistry*, 2007, **11**, 1101-1107.
18. T. Brousse, M. Toupin, R. Dugas, L. Athouël, O. Crosnier and D. Bélanger, *Journal of The Electrochemical Society*, 2006, **153**, A2171-A2180.
19. H. Xia, J. Feng, H. Wang, M. O. Lai and L. Lu, *Journal of Power Sources*, 2010, **195**, 4410-4413.
20. S. Chen, J. Zhu, X. Wu, Q. Han and X. Wang, *ACS nano*, 2010, **4**, 2822-2830.
21. F. Wang, S. Xiao, Y. Hou, C. Hu, L. Liu and Y. Wu, *RSC Advances*, 2013, **3**, 13059.
22. G. Yu, L. Hu, N. Liu, H. Wang, M. Vosgueritchian, Y. Yang, Y. Cui and Z. Bao, *Nano letters*, 2011, **11**, 4438-4442.
23. C. Liu, Z. Yu, D. Neff, A. Zhamu and B. Z. Jang, *Nano letters*, 2010, **10**, 4863-4868.
24. Y. Wang, Z. Shi, Y. Huang, Y. Ma, C. Wang, M. Chen and Y. Chen, *The Journal of Physical Chemistry C*, 2009, **113**, 13103-13107.
25. B. G. Choi, M. Yang, W. H. Hong, J. W. Choi and Y. S. Huh, *ACS nano*, 2012, **6**, 4020-4028.
26. L. Dong, C. Xu, Y. Li, C. Wu, B. Jiang, Q. Yang, E. Zhou, F. Kang and Q. H. Yang, *Adv Mater*, 2015, DOI: 10.1002/adma.201504747.
27. Z. Zhang, F. Xiao, L. Qian, J. Xiao, S. Wang and Y. Liu, *Advanced Energy Materials*, 2014, **4**, 1400064.
28. B. Wei, L. Wang, Q. Miao, Y. Yuan, P. Dong, R. Vajtai and W. Fei, *Carbon*, 2015, **85**, 249-260.
29. Y. He, W. Chen, X. Li, Z. Zhang, J. Fu, C. Zhao and E. Xie, *ACS Nano*, 2013, **7**, 174-182.
30. Z. Fan, J. Yan, T. Wei, L. Zhi, G. Ning, T. Li and F. Wei, *Advanced Functional Materials*, 2011, **21**, 2366-2375.
31. Y. Zhao, W. Ran, J. He, Y. Huang, Z. Liu, W. Liu, Y. Tang, L. Zhang, D. Gao and F. Gao, *Small*, 2015, **11**, 1310-1319.
32. C. Xu, B. Li, H. Du, F. Kang and Y. Zeng, *Journal of Power Sources*, 2008, **180**, 664-670.
33. S. Shi, C. Xu, C. Yang, Y. Chen, J. Liu and F. Kang, *Scientific reports*, 2013, **3**, 2598.
34. L. Dong, C. Xu, Q. Yang, J. Fang, Y. Li and F. Kang, *J. Mater. Chem. A*, 2015, **3**, 4729-4737.
35. L. Dong, F. Hou, Y. Li, L. Wang, H. Gao and Y. Tang, *Composites Part A: Applied Science and Manufacturing*, 2014, **56**, 248-255.
36. L. Dong, Y. Li, L. Wang, F. Hou and J. Liu, *Materials Letters*, 2014, **130**, 292-295.
37. G.-Y. Heo, Y.-J. Yoo and S.-J. Park, *Journal of Industrial and Engineering Chemistry*, 2013, **19**, 1040-1043.
38. S. Storck, H. Bretinger and W. F. Maier, *Applied Catalysis A: General*, 1998, **174**, 137-146.
39. C. Xu, B. Li, H. Du, F. Kang and Y. Zeng, *Journal of Power Sources*, 2008, **184**, 691-694.
40. C. Xu, H. Du, B. Li, F. Kang and Y. Zeng, *Journal of The Electrochemical Society*, 2009, **156**, A73.
41. C. Xu, C. Wei, B. Li, F. Kang and Z. Guan, *Journal of Power Sources*, 2011, **196**, 7854-7859.

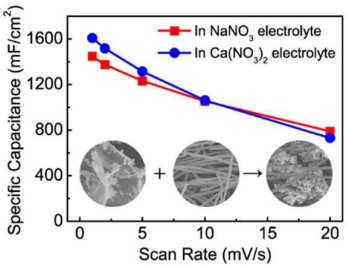

Prepared graphene/MnO_2/activated carbon fiber felt composite textile electrodes are low-cost and have high electrochemical performance in different neutral electrolytes.